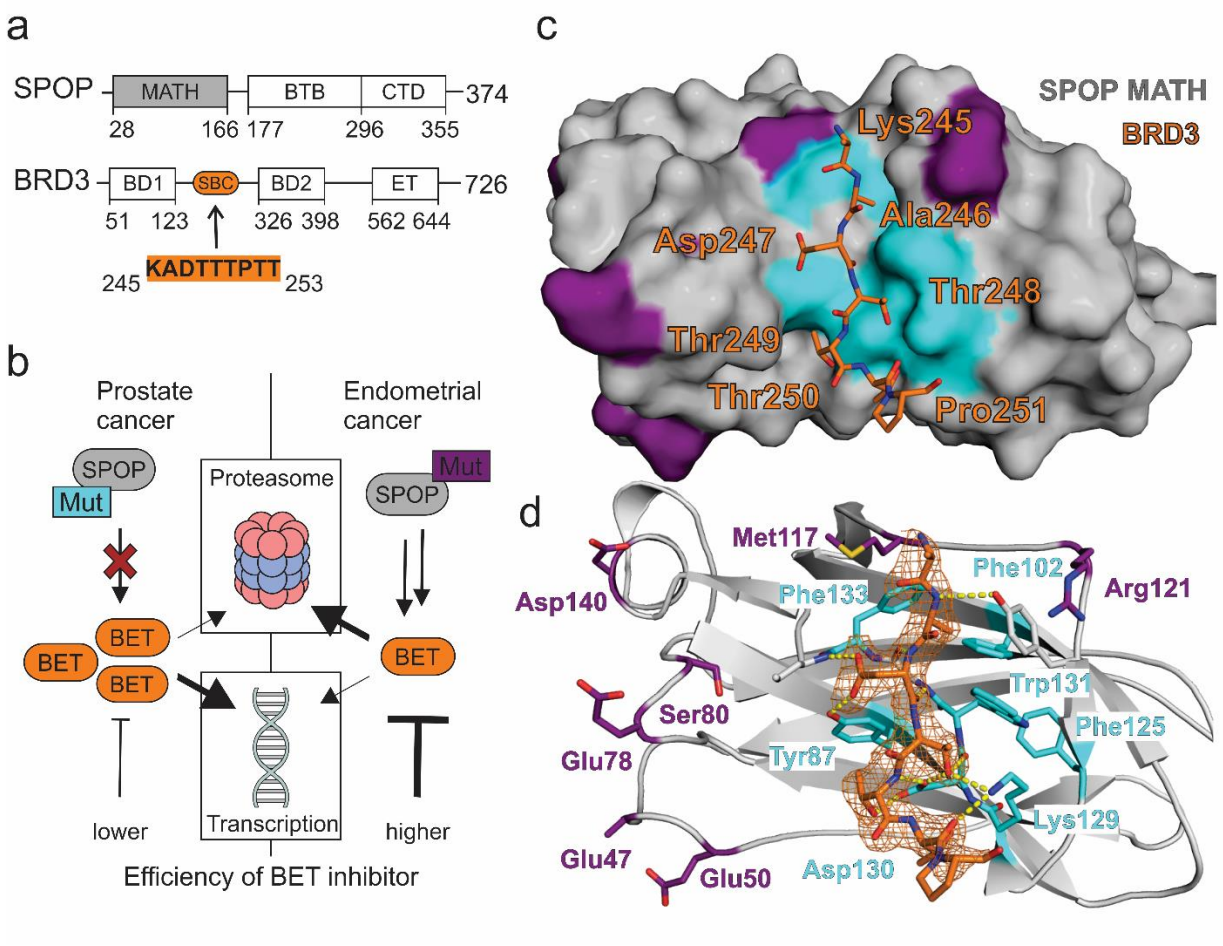

Figure 1. Structure and function of the SPOP-BET complex.

a: Schematic display of SPOP and BRD3 domain architecture.

SPOP contains a MATH domain for substrate binding, and a BTB domain which mediates the interaction to the E3 ubiquitin-ligase cullin-3. It also enables dimerization. The C-terminal domain (CTD) contains an additional dimerization interface. BRD3 contains two bromodomains (BD1 and BD2) and the extraterminal (ET) domain. The SPOP binding consensus (SBC, residues 245-253) is located in an unstructured linker region between the two bromodomains.

b: Cellular pathway of the SPOP-BET protein interaction in prostate and endometrial cancer.

In prostate cancer, SPOP mutations disrupt BET protein binding, which leads to a decreased ubiquitination turnover and diminished BET degradation by the proteasome. The accumulation of BET proteins causes a malignant transcriptional program with decreased drug susceptibility towards BET inhibitors. Contrarily, in endometrial cancer, cellular BET protein levels are diminished, again leading to a malignant transcriptional program, but increasing the drug susceptibility towards BET inhibitors. Lower BET protein levels are presumably caused by increased SPOP binding due to mutation, resulting in increased ubiquitination and proteasomal degradation rates of BET proteins.

c: Surface display of the SPOP-BRD3 co-crystal structure with BRD3 shown as sticks.

SPOP MATH (28-166, wild-type) is shown in grey, BRD3 (**1**, residues 245-253) is shown in orange. SPOP endometrial cancer-associated mutation sites are shown in purple, prostate-cancer associated mutations sites in cyan. BRD3 sits in a shallow groove on the SPOP MATH surface. Prostate cancer associated mutation sites are clustered around the BRD3 binding site, while endometrial cancer associated mutation sites are distant from the binding groove.

d: Cartoon display of the SPOP-BRD3 co-crystal structure with key interactions highlighted.

Electron density for BRD3 is shown as mesh. Hydrogen bonds between SPOP and BRD3 are shown as yellow dashed lines. Cancer associated mutation sites and residues involved in binding are shown as sticks. Prostate cancer associated mutations (cyan) occur in residues directly involved in H-bonds or hydrophobic contacts to the BRD3 ligand, thus disrupting key binding features. This rationalizes the reduced BET protein binding capabilities of prostate cancer associated SPOP mutants on a structural level.

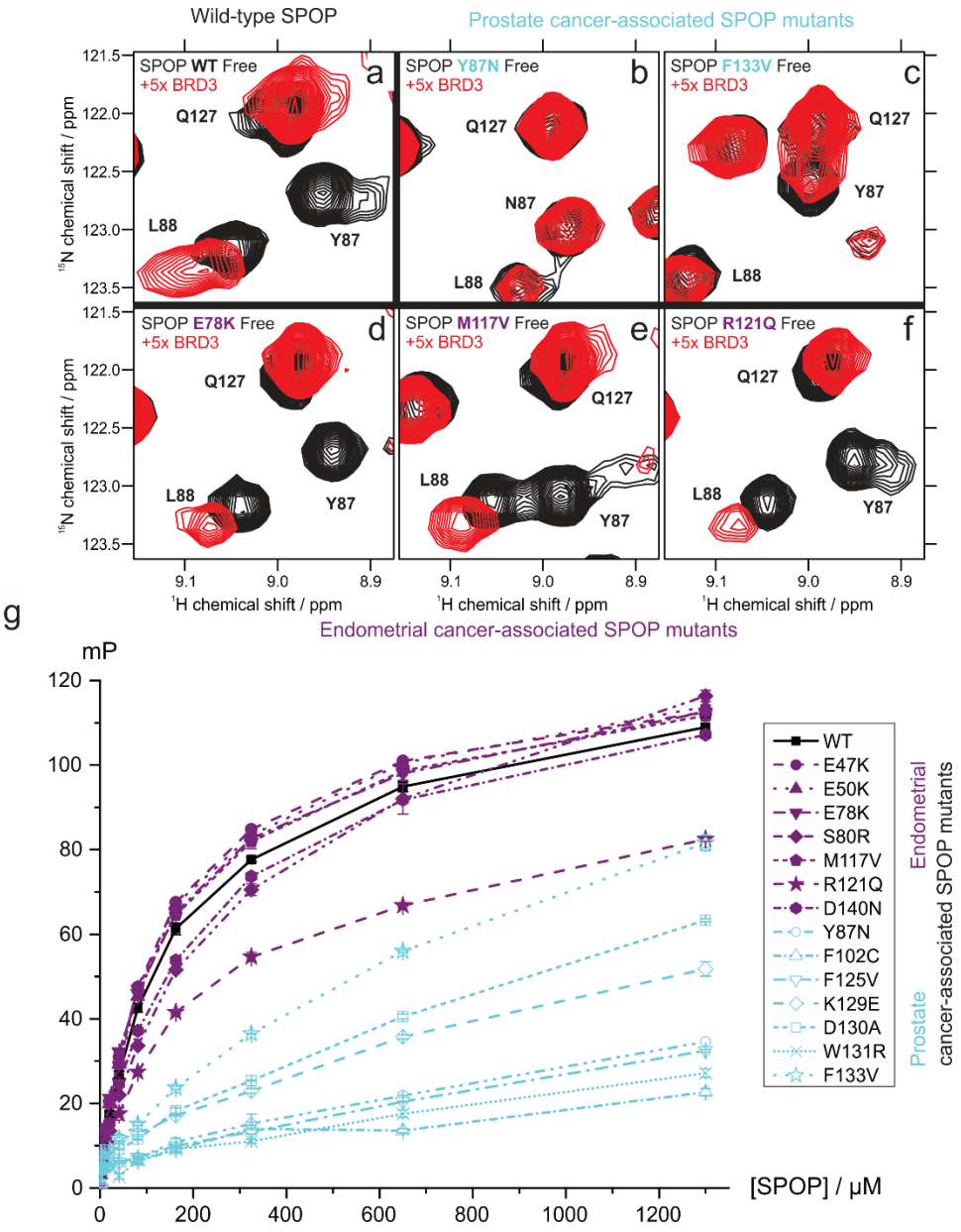

Figure 2. Biophysical analysis of cancer-associated SPOP mutants binding behavior to BRD3.

a-f: Overlays of $^{1}H,^{15}N$ HSQC NMR spectra of selected SPOP mutants titrated with BRD3.

Panels show the reference spectra (free form) in black for the indicated SPOP proteins. Superimposed are spectra recorded after addition of 5x molar excess of BRD3 (**1**, residues 245-253). The wild-type SPOP protein (a) shows clear chemical shift perturbations (CSPs) indicating binding upon addition of BRD3 in peaks corresponding to residues L88 and Q127. The signal for Y87 is broadened beyond detection. These residues are located directly in the BRD3 binding pocket. Selected prostate cancer-associated SPOP mutants Y87N (b) and F133V (c) show no or significantly reduced CSPs compared to the wild type, respectively. This indicates severely reduced binding. Contrarily, endometrial cancer-associated SPOP mutants E78K (d), M117V (e) and R121Q (f) show CSPs comparable to the wild type, indicating similar binding mode and strength. Full spectra are shown in Fig. S1.

g: Fluorescence polarization binding curves of different SPOP mutants to BRD3.

SPOP proteins were mixed in a dilution series with fluorescently labeled BRD3 peptide (**4**). Fluorescence polarization values are displayed as mP units. All curves were normalized to 0. The binding curve of wild-type SPOP to BRD3 is shown in black with square ticks. Out of the endometrial cancer-associated mutants (purple curves), mutants E47K, E50K, E78K, S80R, M117 and D140N show binding strength highly similar to the wild type. Only SPOP R121Q of this group shows slightly reduced BRD3 binding. All prostate cancer associated mutants (cyan curves) show significantly reduced binding to BRD3 compared to SPOP wild type.

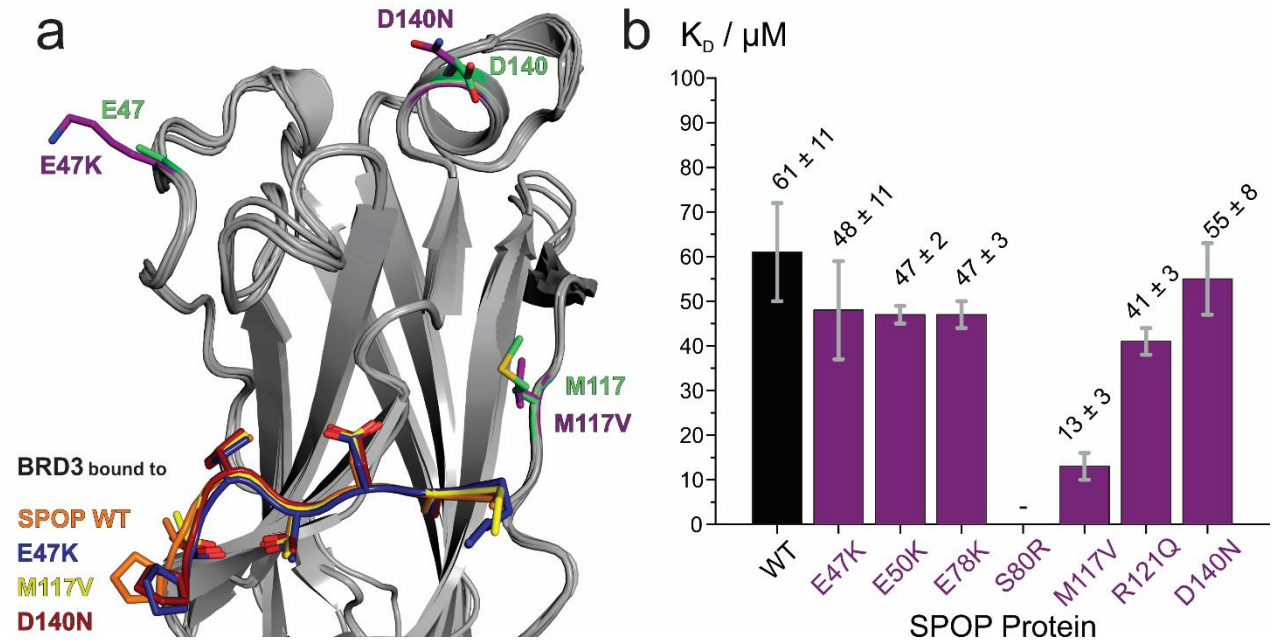

Figure 3a. Overlay of co-crystal structures of different SPOP mutants in complex with BRD3.
The overlay shows one representative complex for each of the co-crystal structures obtained for SPOP wild-type (WT), E47K, M117V and D140N with BRD3 (**1**, residues 245-253). SPOP molecules are shown in grey. Mutation sites E47, M117 and D140 in the SPOP WT-BRD3 co-crystal structure are shown as green sticks. In each of the mutant co-crystal structures, the respective mutated residue (K47, V117 or N140) is shown as purple sticks. The BRD3 ligand from all four co-crystal structures is shown as cartoon with side chains (BRD3 from SPOP WT co-crystal structure in orange, from E47K in blue, from M117V in yellow and from D140N co-crystal structure in red). The overlay shows that all superimposed structures are almost identical in terms of SPOP backbone and BRD3 ligand orientation. This indicates that endometrial cancer associated mutations E47K, M117V and D140 do not alter the interface of SPOP MATH to BRD3.

b: Column plot of K_D values obtained from ITC titrations of different SPOP constructs to BRD3.
The plot shows the K_D values (y-axis) obtained from ITC titrations of different SPOP constructs (x-axis) to the BRD3 protein (residues 24-416). Wild-type SPOP is shown in black. Endometrial cancer-associated SPOP mutants are shown in purple. This is a graphical representation of the numbers given in Table1. For SPOP S80R no data could be obtained due to sample instability.

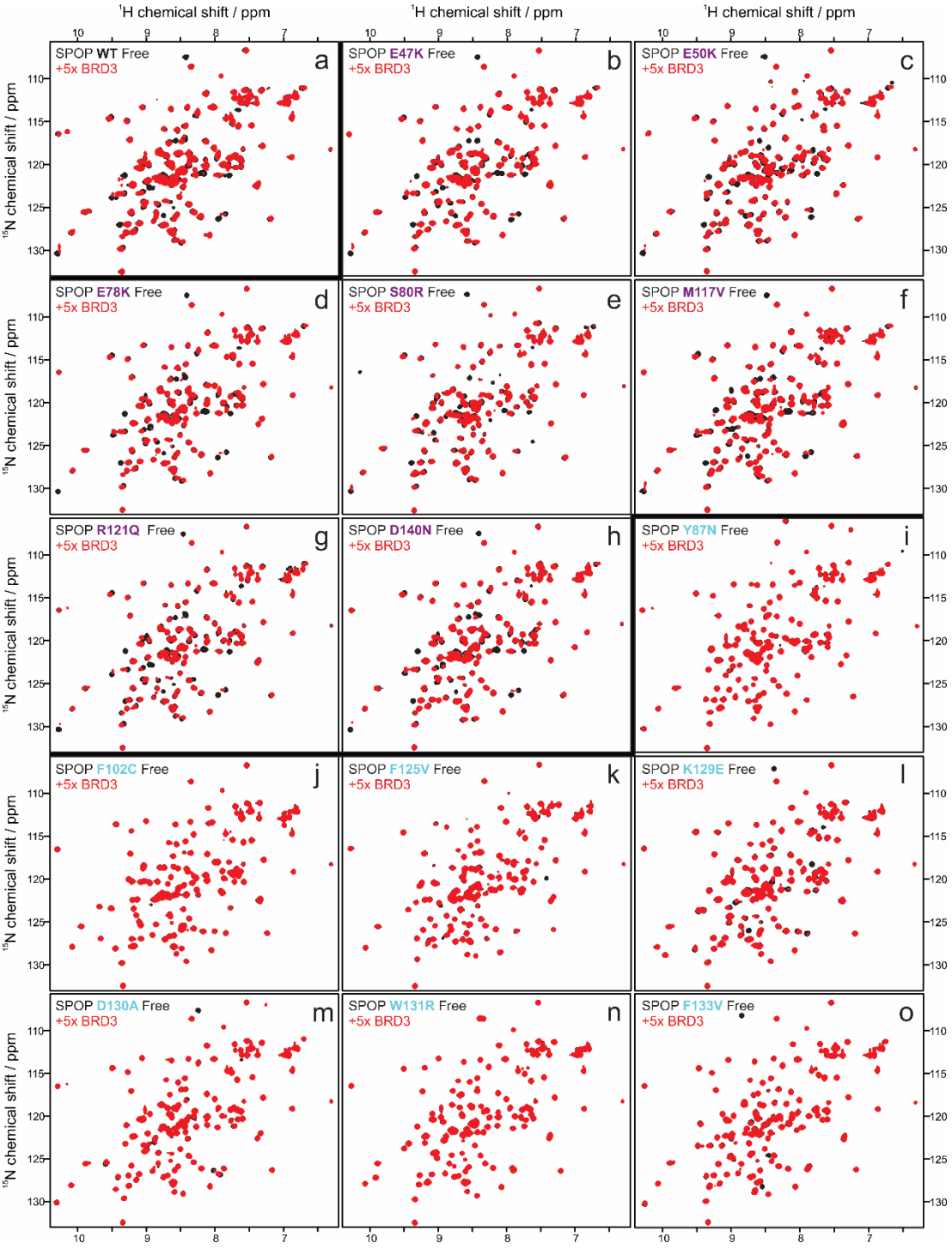

Figure S1. NMR analysis of SPOP-BRD3 binding behavior.

Panels show ^{1}H,^{15}N HSQC NMR spectra of different SPOP MATH proteins. Black spectra represent the respective proteins in free form (without ligand). Red spectra represent samples of SPOP proteins with 5x molar excess of BRD3 (**1**, residues 245-253). Panel a shows the spectra overlay of wild-type SPOP for reference. Panels b-h show spectral overlays of endometrial cancer associated SPOP mutants. Panels i-o show prostate cancer associated mutants. All endometrial cancer mutants show highly similar chemical shift perturbation (CSP) patterns upon BRD3 addition, comparable to wild-type SPOP, indicating a similar binding mode and strength. Contrarily, prostate cancer mutants show no or very little CSPs upon BRD3 addition, indicating no or severely weakened binding, respectively.

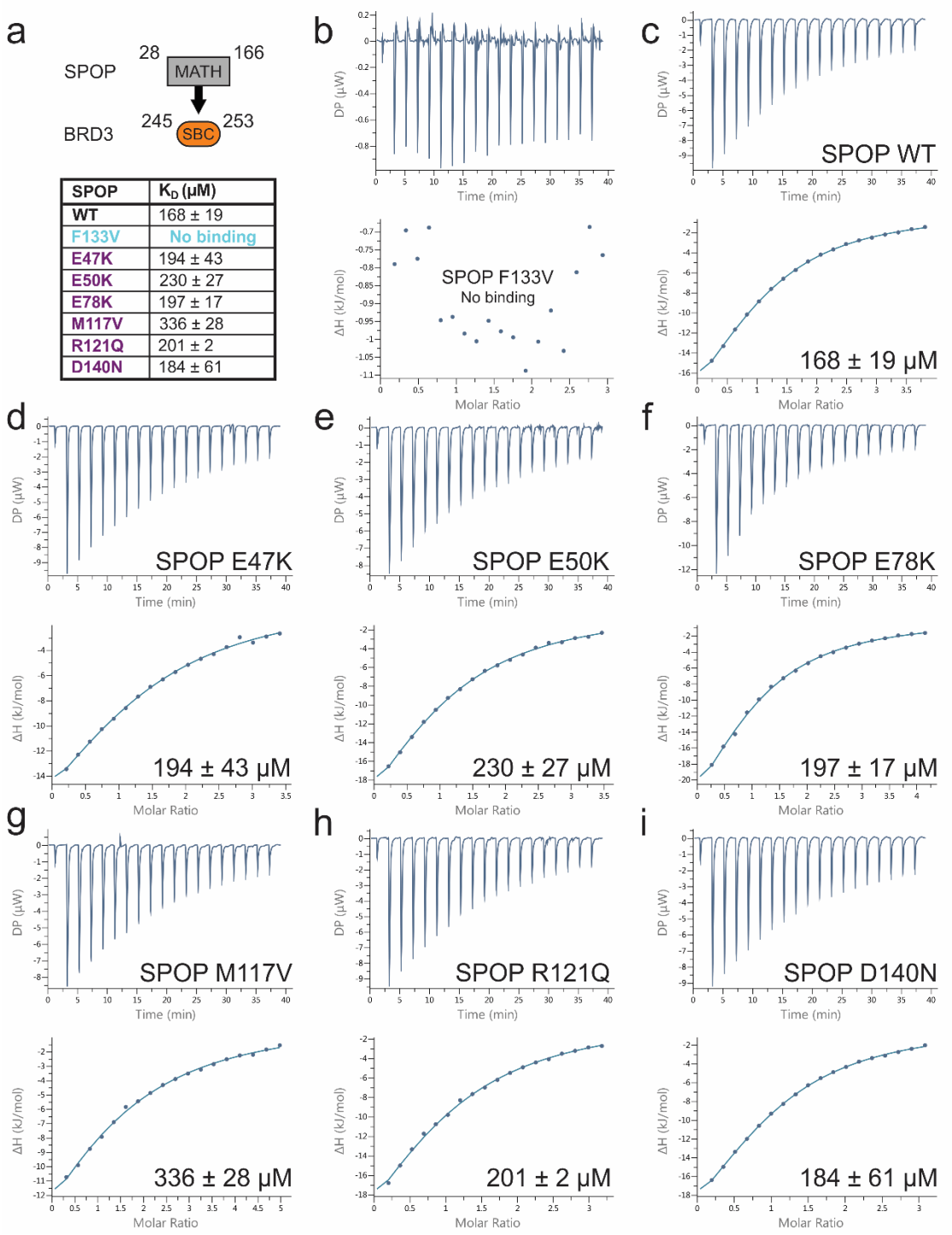

SPOP	K_D (µM)
WT	168 ± 19
F133V	No binding
E47K	194 ± 43
E50K	230 ± 27
E78K	197 ± 17
M117V	336 ± 28
R121Q	201 ± 2
D140N	184 ± 61

Figure S2. ITC data wild-type and cancer-associated SPOP mutants titrated to BRD3 peptide (1, res. 245-253).
Panel a shows a schematic overview of the used constructs. Boundaries and motifs are indicated (MATH: Mephrin and TRAF homology domain, SBC: SPOP binding consensus). The table shows the determined K_Ds with standard deviation for each titrated SPOP protein, calculated from triplicate runs. Panels b-h show representative ITC curves and the determined K_D values for each used SPOP protein. The prostate cancer associated SPOP mutant F133V (b) shows no binding in ITC experiments, whereas wild-type SPOP shows clear binding (c). The endometrial cancer associated SPOP mutants (d-i) show highly similar curve shapes and comparable K_D values to SPOP WT (c), indicating that the mutations do not significantly change BRD3 binding behavior.

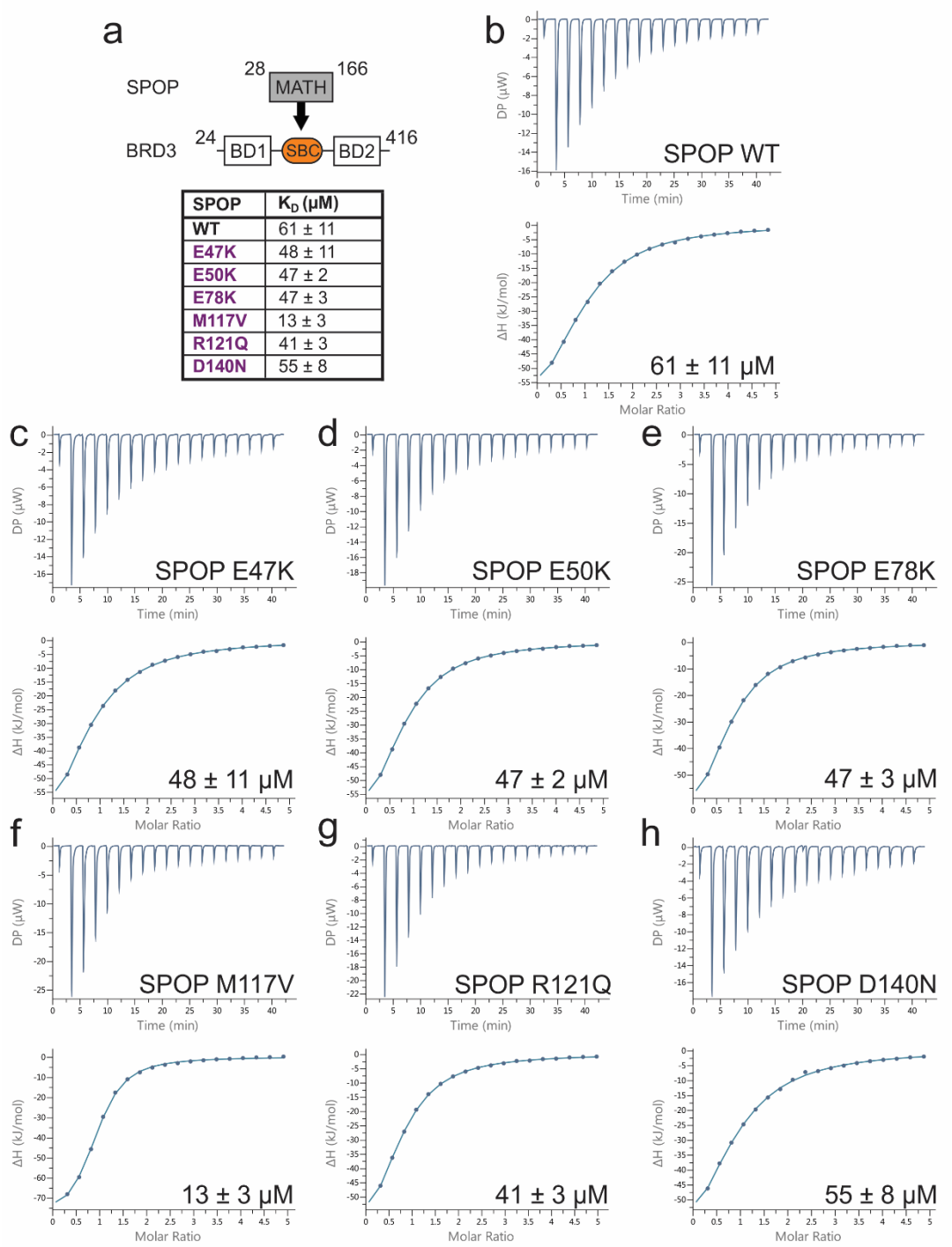

SPOP	K_D (µM)
WT	61 ± 11
E47K	48 ± 11
E50K	47 ± 2
E78K	47 ± 3
M117V	13 ± 3
R121Q	41 ± 3
D140N	55 ± 8

Figure S3. ITC data of wild-type and endometrial cancer associated SPOP mutants titrated to BRD3 protein (residues 24-416) . Panel a shows a schematic overview of SPOP and BRD3 constructs used. The construct boundaries and motifs are indicated (SBC: SPOP binding consensus, BD: Bromodomain). The table shows the obtained K_D values with standard deviations calculated from multiple runs. Panels b-h show representative ITC curves with the determined K_D for each used SPOP protein as indicated. The endometrial cancer associated SPOP mutants E47K (c), E50K (d), E78K (e), R121Q (g) and D140N (h) show highly similar K_D values, which are comparable to SPOP WT (b). Only the mutant M117V (f) shows slightly increased BRD3 affinity. Except for M117V, all endometrial cancer associated SPOP mutations do not show altered BRD3 binding behavior compared to wild-type SPOP.

Table 1: Isothermal titration calorimetry data obtained for titrations of different SPOP constructs to BRD3 protein.
The used SPOP proteins (wild-type (black) or endometrial cancer-associated mutants (purple)) are indicated, as well as the used BRD3 construct. KD is the affinity (dissociation constant), ΔH is enthalpy, ΔG is Gibbs free energy, -TΔS indicates entropy. n is the number of independent experiments used to calculate values and standard deviations. For SPOP S80R, no data could be obtained due to sample instability. With the exception of M117V, all endometrial cancer-associated SPOP mutants show BRD3 binding behavior highly similar to the wild-type.

SPOP protein	BRD3 construct	K_D (μM)	ΔH (kJ/mol)	ΔG (kJ/mol)	-TΔS (kJ/mol)	n
WT	24-416	61 ± 11	-95 ± 13	-24.1 ± 0.4	70 ± 13	3
E47K	24-416	48 ± 11	-85 ± 14	-24.7 ± 0.6	61 ± 15	3
E50K	24-416	47 ± 2	-86 ± 2	-24.7 ± 0.1	61 ± 2	3
E78K	24-416	47 ± 3	-92 ± 1	-24.8 ± 0.1	67 ± 1	3
S80R	-	-	-	-	-	-
M117V	24-416	13 ± 3	-83 ± 2	-27.9 ± 0.5	55 ± 2	6
R121Q	24-416	41 ± 3	-80 ± 1	-25.0 ± 0.2	55 ± 1	3
D140N	24-416	55 ± 8	-102 ± 8	-24.4 ± 0.3	78 ± 8	3

Table S1: Overview of crystallographic data collection and refinement statistics for SPOP-BRD co-crystal structures.

General Information				
PDB ID	**6I41**	**6I5P**	**6I68**	**6I7A**
SPOP variant	residues 28-166 **wild-type**	residues 28-166 **E47K**	residues 28-166 **M117V**	residues 28-166 **D140N**
BRD3 construct	(**1**, residues 245-253)	(**1**, residues 245-253)	(**1**, residues 245-253)	(**1**, residues 245-253)
Data Collection				
Beamline	ESRF ID23-2	ESRF ID30A	ESRF ID30A	ESRF ID30A
Wavelength (Å)	0.8731	0.9660	0.9660	0.9660
Space group	C 1 2 1	P 1 21 1	P 1 21 1	P 41 21 2
Cell dimensions				
a,b,a (Å)	61.507, 55.180, 42.606	44.962, 90.334, 88.863	44.775, 90.128, 88.563	90.351, 90.351, 166.591
α,β,γ (°)	90.000, 100.394, 90.000	90.000, 91.190, 90.000	90.000, 91.170, 90.000	90.000, 90.000, 90.000
Resolution range (Å)	1.79 - 40.80	1.71 - 45.17	1.75 - 90.13	1.95 - 8.72
Observed reflections	85563	243977	215636	433522
Unique reflections	13067	75547	70332	51096
Whole range				
Completeness (%)	98.3	98.6	99.2	99.9
R_{meas} (%)	9.5	5.8	5.4	7.0
I/σ (I)	9.8	11.82	10.9	14.71
Last shell				
Resolution (Å)	1.79	1.71	1.75	1.95
Completeness (%)	83.8	98.5	95.6	98.9
R_{meas} (%)	84.3	136.8	76.0	262.5
I/σ (I)	1.50	1.16	1.50	0.83
Refinement Statistics				
No. of reflections	11029	63697	59532	48938
Resolution (Å)	1.90	1.81	1.85	2.20
R-factor (%)	19.2	19.0	19.8	20.0
R_{free} (%)	23.8	22.7	23.8	23.4
Average B ($Å^2$)	38.3	42.0	39.0	59.8
RMSD of bond length (Å)	0.006	0.010	0.006	0.003
RMSD of angles (°)	0.772	1.053	0.823	0.559
Content of asymmetric unit				
No. of protein complexes	1	4	4	4
No. of protein atoms	1077	4478	4533	4415
No. of solvent atoms	132	486	472	261

Table S2: Isothermal titration calorimetry data obtained for titrations of different SPOP constructs to BRD3-derived peptides. The used SPOP proteins (wild-type (black), prostate cancer-associated SPOP mutants (cyan) or endometrial cancer-associated mutants (purple)) are indicated, as well as the used BRD3 construct. K_D is the affinity (dissociation constant), ΔH is enthalpy, ΔG is Gibbs free energy, -TΔS indicates entropy. n is the number of independent experiments used to calculate values and standard deviations. Prostate cancer-associated SPOP mutant F133V shows no binding in ITC experiments. Endometrial cancer-associated mutants show binding comparable to wild-type SPOP. For SPOP S80R, no data could be obtained due to sample instability.

SPOP protein	BRD3 construct	K_D (μM)	ΔH (kJ/mol)	ΔG (kJ/mol)	-TΔS (kJ/mol)	n
WT	245-253	168 ± 19	-27 ± 5	-21.6 ± 0.3	5.7 ± 5	3
F133V	245-253	**no binding**	-	-	-	3
E47K	245-253	194 ± 43	-24 ± 3	-21.3 ± 0.5	2.4 ± 3.5	3
E50K	245-253	230 ± 27	-40 ± 3	-20.8 ± 0.3	20 ± 4	3
E78K	245-253	197 ± 17	-45 ± 6	-21.2 ± 0.2	24 ± 7	3
S80R	-	-	-	-	-	-
M117V	245-253	336 ± 28	-26 ± 2	-19.8 ± 0.2	6 ± 2	3
R121Q	245-253	201 ± 2	-36 ± 1	-21.1 ± 0.1	15 ± 1	3
D140N	245-253	184 ± 61	-33 ± 10	-21.5 ± 0.8	12 ± 11	3